IEEE Access
Multidisciplinary : Rapid Review : Open Access Journal

Received July 27, 2019, accepted August 17, 2019, date of publication August 27, 2019, date of current version September 11, 2019.

Digital Object Identifier 10.1109/ACCESS.2019.2937847

Fuzzy-Type Fast Terminal Sliding-Mode Controller for Pressure Control of Pilot Solenoid Valve in Automatic Transmission

XIANGWEN FAN[1], **YONGYI HE**[1,2], **PENGFEI CHENG**[1], **AND MINGLUN FANG**[1,2]

[1]Institute of Mechanical and Electronic Engineering and Automation, Shanghai University, Shanghai 200439, China
[2]Shanghai Key Laboratory of Intelligent Manufacturing and Robotics, Shanghai University, Shanghai 200439, China

Corresponding author: Xiangwen Fan (fxw1212@163.com)

This work was supported by the Projects Foundation of the Shanghai Science and Technology Commission, China, under Grant 17511104602.

ABSTRACT The performance of the pilot solenoid valve (PSV) has a significant impact on the efficiency and service life of an automatic transmission (AT) in automobiles, and it is very difficult to achieve a perfect pressure tracking performance due to the sophisticated combination of mechanical, hydraulic and electromagnetic characteristics inside the PSV. In this paper, based on a nominal nonlinear dynamic model of the PSV including uncertainties and an external disturbance, a fast terminal sliding-mode control (FTSMC) method is developed to achieve tracking precision and robustness in the pressure control of the PSV. To alleviate the chattering phenomenon in the control input signal, fuzzy logic rules are established to tune the switching control coefficient of the control law in FTSMC controller. Compared with the trend-law-based sliding-mode control (TLSMC) method and PID method, the developed fuzzy-type fast terminal sliding-mode control (F-FTSMC) method achieves the shortest settling time, the smallest tracking error at steady state and almost no chattering in the control input by intelligently changing the control law. Simulations and experiments are demonstrated to verify the effectiveness and excellent advantages of the proposed controller.

INDEX TERMS Fast terminal sliding mode control, fuzzy control, pressure control, pilot solenoid valve, automatic transmission.

I. INTRODUCTION

An automatic transmission (AT) is widely adopted in automobiles because of its superiority in continuous power shifting and self-adjustment capability [1]. As one of the lower-level actuators of the electrical control unit (ECU), the pilot solenoid valve (PSV) receives a shift command from the ECU, and controls the system pressure to move the shift spool for automatic shifting in the AT. Thus, the PSV must have a fast, precise and stable response to the command from the ECU to ensure an optimum quality of the shift of the AT. However, pressure control of the PSV is complicated because its dynamic characteristic arises from three different systems: the mechanical system of the spool and spring, the electromagnetic system of the solenoid and the hydraulic system of the fluid [2]. In addition, the harsh working environment also has a great impact on the pressure control. There exist various nonlinear factors, such as electromagnetic and friction force, and parameter uncertainties and external disturbances, such as the return-spring limp-home and the effect of the flow rate. In summary, the development of an excellent control method for pressure control of the PSV is very valuable.

Most research on solenoid valves has focused on modeling and simulating the effect of their internal structural parameters on the valve performance [2]–[5] and further optimizing the valve structure [5]–[9]. Although some studies have discussed the output control of the solenoid valve, in most studies, the valve is just considered as a part of a system, such as an electro-hydraulic control load system [10], a pneumatic force-feedback system for an arm-exoskeleton [11] and others in [12]–[14]. The research emphasis in these studies was system control, not control of the valve. Therefore, the valve control models were greatly simplified and could not truly express the nonlinearity inside the valve.

The associate editor coordinating the review of this article and approving it for publication was Yanzheng Zhu.

Few studies have focused on an output control method for a solenoid valve based on a detailed nonlinear dynamic model. In [15], for quick and precise pressure control of a proportional pressure solenoid valve (PPSV) in a dual-clutch transmission (DCT), a triple-step method was used to design a nonlinear controller based on a controller-oriented model of the PPSV. A flatness based feedback control method for an automotive solenoid valve was studied to provide a convenient control framework for meeting many performance specifications on the end motion of valve incorporating voltage constraints, nonlinear magnetic effects and various motion uncertainties in [16]. In [17]–[19], valves were controlled by different nonlinear controllers considering various influencing factors. Among the nonlinear control methods similar to the above studies, establishing an accurate mathematical control model of a valve is difficult but essential, and the control robustness cannot be perfectly guaranteed under time-varying uncertainties and an external disturbance.

In recent years, due to its intrinsic robustness to uncertainties and external disturbances, the variable structure with sliding-mode control (SMC) has gradually become one of the important control methods for very complex nonlinear systems. The method was proposed originally by Utkin [20]. Different from the traditional SMC method in which a linear sliding surface function is adopted and the deviation between the system state and the given trajectory is asymptotically convergent, terminal sliding-mode control (TSMC) improves the convergence characteristics by introducing a nonlinear term in the sliding surface function, and the system state can converge to a given trajectory in a finite time [21]. In [21]–[23], it was proven that a TSMC controller can exhibit strong robustness to system parameter uncertainties and external disturbances since the sliding-mode motion is independent of these effects. However, sliding-control method will cause chattering in the control input of the system due to its inherent discontinuous switching characteristics, and some methods must be used to reduce this chattering. For example, in [22], a robust adaptive TSMC controller was developed by limiting the control inputs despite the presence of inertia uncertainties and unknown external disturbances. In fact, research on anti-chattering in SMC controller has attracted increasing interests, and many studies have proposed solutions from the perspective of controller design. In [24], [25], researchers either changed the switching function or changed the thickness of the boundary layer to effectively reduce the chattering by a quasi-sliding-mode controller (Q-SMC). In [26], [27], filters of various structures were designed to smooth the control input signal to reduce the chattering. In [28], [29], state observers were used to eliminate uncertainties and external disturbances because they are the main source of chattering in SMC controllers. In practical applications, intelligent algorithms such as fuzzy logic algorithms [30], [31], neural network algorithms [32], [33] and genetic optimization algorithms [34], [35] are popular because of their simple structures and fewer parameters. These algorithms can be used to approximate the nonlinear part of the SMC controller or directly implement on SMC control due to their strong nonlinear approximation and smoothing ability.

Currently, an improved SMC controller is usually used to control the actuator in a system that includes valves. With this controller, the relationship between the input and the output of the valve itself cannot be shown exactly. In this paper, a fuzzy-type fast terminal sliding-mode control (F-FTSMC) method is developed to study the relationship between the input voltage signal and output pressure. A fuzzy logic controller is adopted to tune the switching control coefficient of the TSMC controller and, as a result, mitigate the chattering of the control input signal. In addition, to compensate for the time spent due to querying fuzzy rules, a fast terminal sliding surface function can be chosen in the TSMC controller to speed up the convergence time of the sliding motion [36]. The rest of this paper is organized as follows: Sect. 2 provides detailed descriptions of the nominal dynamic nonlinear model of the PSV. The proposed F-FTSMC controller is described in Sect. 3. Simulations are implemented and the results are discussed for two cases in Sect. 4. In Sect. 5, experimental results are shown to verify the advantages of the proposed controller. Finally, the conclusions are summarized in Sect. 6.

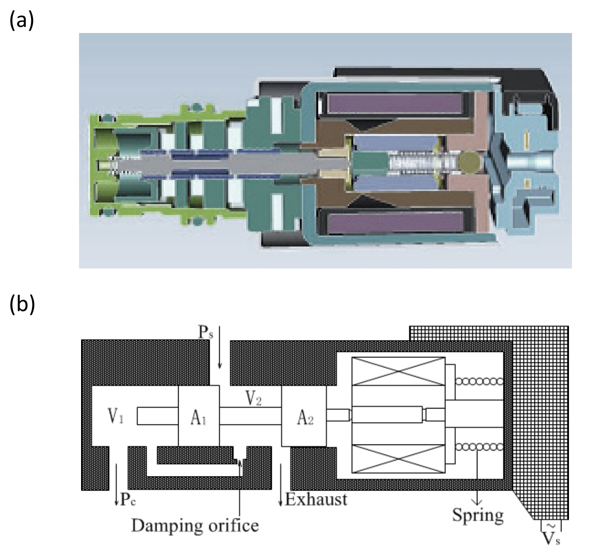

FIGURE 1. Pilot solenoid valve: (a) Sectional drawing. (b) Equivalent diagram.

II. NOMINAL DYNAMIC MODEL OF PSV

A sectional drawing and equivalent diagram of the PSV studied in this paper are shown in Fig. 1. The supply pressure (P_s) is compressed in chamber 1 (V_1) and chamber 2 (V_2) through a damping orifice. The input voltage (V_s) generates the electromagnetic force to move the spool that slides in the valve horizontally to adjust the flow rate and pressure. The spring is used to react to the movement of the spool. It can be easily seen from Fig. 1 that the valve comprises fluid dynamics, mechanical dynamics and electromagnetic dynamics.

The movement of the spool is balanced by the fluid pressure force F_p, spring force F_s, friction force F_r and electromagnetic force F_{em}, which can be described based on Newton's second law [5]:

$$F_p + F_{em} + F_s + F_r = m_v \ddot{x_v} + d_v \dot{x_v} \tag{1}$$

where m_v represents the equivalent mass of the valve spool, $x_v < x_{max}$ is the displacement of the spool, and x_{max} is 7.8 mm in this paper. The damping coefficient of the valve damping orifice is d_v.

F_p is the control pressure acting on the left of the spool in V_1, and which can be expressed as:

$$F_p = P_c A_1 \tag{2}$$

where P_c is the control pressure of the valve, and A_1 is the area of the left end on the spool.

The electromagnetic force of the solenoid valve is actuated by the applied voltage and can be expressed by simplified as [3], [6]:

$$F_{em} = -\frac{k_f L}{R} u \tag{3}$$

where k_f is the gain coefficient of the electromagnetic force, L and R are the equivalent inductance and resistance of the coil, respectively, and $u = V_s$ is the control input voltage.

The spring force acting on the spool can be described as:

$$F_s = -k(x_0 + x_v) \tag{4}$$

where k is the spring constant, and x_0 is the initial compression of the valve spring.

The friction force considered here comprises the viscosity friction force and static friction force, and the equation of the friction force can be described as [2]:

$$F_r = -f_R \dot{x_v} - f_s sign(\dot{x_v}) \tag{5}$$

where f_R and f_s are the viscosity friction coefficient and the static friction coefficient, respectively. $sign(\dot{x_v})$ is a symbolic function.

In addition, the following expression can be derived by applying the continuity equation to chamber V_1 [13]:

$$\frac{\dot{P_c} V_1}{\beta_v} = Q_s - Q_{ex} - A_1 \dot{x_v} \tag{6}$$

where Q_s and Q_{ex} are the supply flow rate and exhaust flowrate of the valve, respectively. β_v is the effective bulk modulus, which varies because of the changes in pressure and temperature.

To summarize the overall dynamic control model of the PSV, expressions (1) and (6) are combined with expressions (2)-(5) by eliminating x_v considering the mechanical dynamics, fluid dynamics and electromagnetic dynamics together. The equation is eventually yielded as follows:

$$\frac{k_f L}{R} u = \frac{d_v V_1}{\beta_v A_1} \ddot{P_c} + \frac{m_v V_1}{\beta_v A_1} \dot{P_c} + A_1 P_c + F_s + F_r + \frac{m_v (Q_s - Q_{ex})}{A_1} \tag{7}$$

For obtain the nominal model of valve, expression (7) can be rewritten simply as [14]:

$$a\ddot{P_c} + b\dot{P_c} + cP_c + F_{sn} + F_{rn} + F_{qn} = u \tag{8}$$

where

$$\begin{aligned} a &= \frac{d_v V_1 R}{\beta_v A_1 k_f L}, \quad b = \frac{m_v V_1 R}{\beta_v A_1 k_f L}, \\ c &= \frac{A_1 R}{k_f L}, \quad F_{sn} = \frac{-kR(x_0 + x_v)}{k_f L}, \\ F_{rn} &= \frac{-R[f_R \dot{x_v} + f_s sign(\dot{x_v})]}{k_f L}, \\ F_{qn} &= \frac{m_v R (Q_s - Q_{ex})}{A_1 k_f L} \end{aligned} \tag{9}$$

The vibration caused by a flow rate variation usually has a greater influence on the performance of the solenoid valve than the flow rate itself, and when the supply flowrate Q_s is determined, the value of F_{qn} generally fluctuates within a small certain range. Thus, F_{qn} will be considered to be a part of the external disturbances later and is not included in the uncertainties of the valve here. As a result, the uncertainties above can be expressed as:

$$\begin{aligned} a &= a_0 + \Delta a, \quad b = b_0 + \Delta b, \quad c = c_0 + \Delta c, \\ F_{sn} &= F_{sn0} + \Delta F_{sn}, \quad F_{rn} = F_{rn0} + \Delta F_{rn} \end{aligned} \tag{10}$$

where $a_0 = \frac{d_v V_{10} R_0}{\beta_{v0} A_1 k_f L_0}$, $b_0 = \frac{m_v V_{10} R_0}{\beta_{v0} A_1 k_f L_0}$, $c_0 = \frac{A_1 R_0}{k_f L_0}$, V_{10}, R_0, β_{v0}, and L_0 are the nominal values of the valve parameters. $F_{rn0} = \frac{-R_0[f_R \dot{x_v} + f_s sign(\dot{x_v})]}{k_f L_0}$, and $F_{sn0} = \frac{-kR_0(x_0 + x_v)}{k_f L_0}$ are the nominal values of friction force and spring force. Δa, Δb, Δc, $\Delta F_{sn} = \Delta_1 + \Delta_2 x_v$, $\Delta F_{rn} = \Delta_3 \dot{x_v} + \Delta_4 sign(\dot{x_v})$ denote the unknown bounded uncertainties of the control parameters of the valve. So, expression (8) can be written as:

$$a_0 \ddot{P_c} + b_0 \dot{P_c} + c_0 P_c + F_{sn0} + F_{rn0} = u + F_{lum} \tag{11}$$

where F_{lum} represents the lumped uncertainty of the PSV and is bounded by a constant δ. By combining expression (8) and (11), it can be derived as:

$$\begin{aligned} &F_{lum} = F_{qn} - \Delta a \ddot{P_c} - \Delta b \dot{P_c} - \Delta c P_c - \Delta F_{sn} - \Delta F_{rn} \\ &|F_{lum}| \le \delta, \quad (\delta > 0) \end{aligned} \tag{12}$$

Finally, the nominal model of the PSV can be given as:

$$a_0 \ddot{P_c} + b_0 \dot{P_c} + c_0 P_c + F_{sn0} + F_{rn0} = u_{nom} \tag{13}$$

where u_{nom} is the nominal control signal.

Remark 1: It is easily seen from expression (12) that the lumped uncertainty of the PSV is complicated, consisting of the parameter uncertainties of the valve and the estimation errors of the effective bulk modulus, spring force and friction force. The flow rate variation will also be included in the external disturbance, which is discussed later in this paper. It exhibits complex nonlinear dynamics in the pressure control of the PSV because of the sophisticated combination of mechanical, electromagnetic and hydraulic characteristics.

Considering these factors, it is very difficult for linear control algorithms to obtain a sufficiently perfect performance. Among the nonlinear control methods, the TSMC controller is usually a popular choice. The TSMC controller has a very good ability to handle nonlinearities and good robustness to uncertainties and external disturbances. However, the inherent chattering characteristics make it very challenging to use this controller.

III. F-FTSMC SCHEME

The fast terminal sliding-mode control (FTSMC) method can make the system state converge gradually in a finite time by quickly approaching the equilibrium state of the sliding-mode motion. The control law of the FTSMC controller in this paper is designed based on the switching control method and the equivalent control method. The switching control method is utilized in many classes of systems or issues, such as a stochastic switching system or a piecewise affine system. However, due to factors such as the system inertia, system delay or measurement error, a high-frequency chattering often occurs with the FTSMC controller, which will significantly affect the dynamic performance of the valve. To alleviate this chattering phenomenon, fuzzy logic rules are designed in this section to tune the switching control of the FTSMC controller. Finally, to accelerate the settling process of the pressure control and mitigate the chattering of the control input in the PSV with a lumped uncertainty and external disturbance, the F-FTSMC controller is proposed.

A. FTSMC CONTROLLER

Firstly, the tracking error between the actual output pressure P_c and the reference pressure P_r of the PSV is defined as:

$$e_p = P_c - P_r \tag{14}$$

Given the system model in (11) and taking the second derivative of e_p, we have the tracking error dynamics of the PSV pressure as:

$$\ddot{e}_p = \frac{u + F_{lum} - F_{sn0} - F_{rn0} - b_0(\dot{e}_p + \dot{P}_r)}{a_0} - \ddot{P}_r \tag{15}$$

For robust control of the PSV, the following sliding surface is adopted to represent the terminal sliding mode [29], [36]:

$$s = \dot{e}_p + c_1 e_p + c_2 e_p^{q/p} \tag{16}$$

where c_1 and c_2 are design parameters of FTSMC controller, $c_1 > 0$, and $c_2 > 0$. Besides, q and p are both positive odd numbers and satisfy $q < p < 2q$.

Lemma 1: Assume that the system state reaches the sliding surface, that is, $s = 0$ in expression (16). Then, the time spent from $e_p \neq 0$ to $e_p = 0$ is:

$$t_{e_p} = \frac{p}{c_1(p-q)} \ln \frac{c_1 e_p^{1-q/p} + c_2}{c_2} \tag{17}$$

Proof: $s = 0$ means that:

$$\dot{e}_p + c_1 e_p + c_2 e_p^{q/p} = 0 \tag{18}$$

It can be rewritten as

$$e_p^{-q/p}\dot{e}_p + c_1 e_p^{1-q/p} = -c_2 \tag{19}$$

In order to simplifying the calculation, let $w = e_p^{1-q/p}$, then, expression (19) changes to:

$$\dot{w} + \frac{p-q}{p} c_1 w = -c_2 \frac{p-q}{p} \tag{20}$$

When $e_p = 0$, w is equal to 0, and the time is defined as $t = t_{e_p}$, the result of solving the differential equation (20) is:

$$\frac{c_2}{c_1} e^{-\frac{p-q}{p} c_1 t_{e_p}} + w(0) e^{-\frac{p-q}{p} c_1 t_{e_p}} = -\frac{c_2}{c_1} \tag{21}$$

where $w(0)$ is the initial value corresponding to $e_p(0)$. Take the logarithm of both sides of expression (21):

$$T_{e_p} = \frac{p}{c_1(p-q)} \ln \frac{c_1 w(0) + c_2}{c_2} \tag{22}$$

Substituting $w(0) = e_p(0)^{1-q/p}$ yields:

$$t_{e_p} = \frac{p}{c_1(p-q)} \ln \frac{c_1 e_p(0)^{1-q/p} + c_2}{c_2} \tag{23}$$

which completes the proof of the lemma.

Theorem 1: The system state will arrive at the sliding surface and the pressure tracking error e_p will converge to zero in finite time if the control law of the FTSMC controller is designed as [37], [38]:

$$u = u_{eq} + u_n \tag{24}$$

that

$$\begin{aligned} u_{eq} &= (b_0 - a_0 c_1)\,\dot{e}_p - \frac{a_0 c_2 q}{p} e_p^{\frac{q}{p}-1} \dot{e}_p \\ &\quad + a_0 \ddot{P}_r + b_0 \dot{P}_r + F_{sn0} + F_{rn0} \\ u_n &= -(\delta + \gamma)\,\mathrm{sgn}(s) \end{aligned} \tag{25}$$

where δ is the upper bound of the lumped uncertainties mentioned above, γ is a control parameter, and $\gamma > 0$. Here, u_{eq} represents the equivalent control part and is used to maintain the system state on the sliding surface, and u_n denotes the switching control part and is used to force the system state to slide over the sliding surface.

Proof: Consider a Lyapunov function $V = s^2/2$ and its time derivative along (15-16, 24-25):

$$\begin{aligned} \dot{V} &= s\dot{s} \\ &= s\left(\ddot{e}_p + c_1\dot{e}_p + \frac{c_2 q}{p} e_p^{\frac{q}{p}-1}\dot{e}_p\right) \\ &= \frac{s}{a_0}[u - F_{sn0} - F_{rn0} \\ &\quad - a_0\left(\ddot{P}_r - c_1\dot{e}_p - \frac{c_2 q}{p} e_p^{\frac{q}{p}-1}\dot{e}_p\right) + F_{lum}] \\ &= \frac{s}{a_0}\left[F_{lum} - (\delta+\gamma)\mathrm{sgn}(s)\right] \\ &= \frac{|s|}{a_0}(|F_{lum}| - \delta) - \frac{1}{a_0}\gamma\,|s| \\ &\leq -\frac{1}{a_0}\gamma\,|s| < 0, \quad (\forall\,|s| \neq 0) \end{aligned} \tag{26}$$

in which $|F_{lum}| - \delta \leq 0$ can be easily obtained. Expression (26) implies that the system state will arrive at the sliding surface in a finite time, and this finite time can be expressed as:

$$t_s = -\frac{a_0}{\gamma}\sqrt{2}\left|V(0)^{1/2}\right| \tag{27}$$

Thus, pressure tracking error of the valve will quickly converge to zero on the sliding surface in a finite time t_R, and

$$t_R = t_{e_p} + t_s \tag{28}$$

Remark 2: The FTSMC controller easily causes chattering due to defects of the sliding-mode variable structure itself, which not only affects the accuracy of the system control, but also excites the high-frequency unmodeled part of the system and eventually destroys the system control performance. In this paper, a set of fuzzy logic rules based on equivalent control and switching control is proposed to efficiently weaken the chattering phenomenon in the control input. The basic purpose is to compensate for the influence of the unmodeled part by adjusting the control law in the approaching process of the FTSMC controller in real time, and to ensure that the pressure will quickly track the desired value with less chattering and strong robustness to uncertainties and external disturbances.

B. FUZZY LOGIC RULES

Due to the principle of the FTSMC controller, which consists of equivalent control and switching control, the fuzzy logic as follows: If s is zero then the control law is just the equivalent control u_{eq}; if s is not zero then the control law changes to $u_{eq} + u_n$, which combines equivalent control and switching control. So to reduce the chattering phenomenon, the control law of the F-FTSMC controller is modified by anti-fuzzification method as:

$$u = u_{eq} + \mu_N u_n \tag{29}$$

where μ_N is added as the switching control coefficient and the chattering will be weakened by tuning its value. The amplitude of u is adjusted by a change of μ_N, thereby reducing the chattering of the control input, especially near the sliding surface. In addition, it can reduce the effect of improper selection of the upper bounds δ and the control parameter γ to a certain extent. We choose the sliding variable s as the input of the fuzzy logic controller, and the output is μ_N. The fuzzy subset of both input and output variables is $\{N\,Z\,B\}$, and these linguistic values are: N-negative big, Z-zero, and B-positive big. The degree of the membership functions of two variables are shown in Fig. 2.

The inference rule is: If variable s is away from the sliding surface, a larger μ_N is required to speed up the approach process; if variable s is close to the sliding surface, a smaller μ_N should be selected to reduce the chattering. The rule base used in this paper is presented in Table 1. In addition, the centroid method will be used for defuzzification in this study.

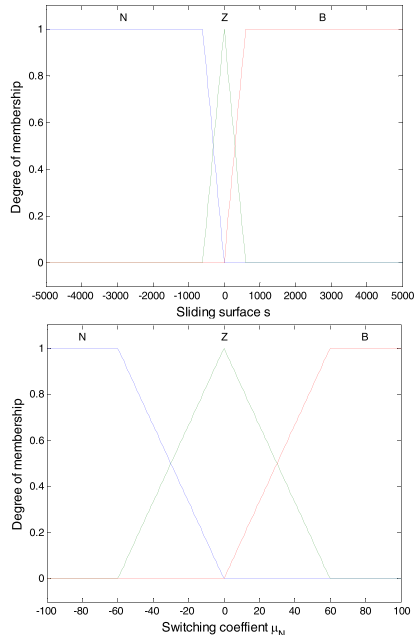

FIGURE 2. Membership functions of s and μ_N.

TABLE 1. Rule base of fuzzy controller.

Rule number	Value of s	Value of μ_N
R1	N	B
R2	Z	Z
R3	B	B

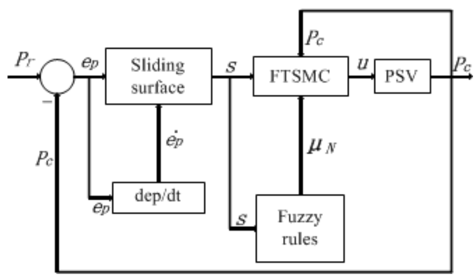

FIGURE 3. Diagram of proposed F-FTSMC scheme.

C. F-FTSMC CONTROLLER

Finally, a diagram of the proposed F-FTSMC controller for pressure control of the PSV is established and shown in Fig. 3 As stated above, fuzzy logic rules are used to tune the switching control coefficient μ_N in the FTSMC controller according to the value of s, and the control input u of the PSV is given by the FTSMC controller. The excellent performance of the developed controller will be validated by simulation end experimental case studies in Sections 4 and 5, respectively.

IV. SIMULATION RESULTS AND DISCUSSION

To demonstrate the effectiveness and advantages of the proposed F-FTSMC controller, simulations for pressure

TABLE 2. Nominal parameters of PSV.

Parameter	Value	Unit	Parameter	Value	Unit
V_{10}	4.86π	(mm^3)	k_f	3.5	
R_0	5.0	(Ω)	m_v	0.195	(kg)
β_{v0}	45×10^7	(N/m^2)	A_1	0.36π	(mm^2)
L_0	3.6	(mH)	f_R	90	$(N \cdot s/m)$
x_0	0.52	(mm)	f_s	0.15	$(N \cdot s/m)$
k	7000	(N/m)	δ	30	
d_v	0.4	$(kg \cdot s/cm^5)$			

control of the PSV are carried out in MATLAB/Simulink. Here, we choose two kinds of reference commands P_r: (1) step signals with changing amplitudes from 0 to 100 kPa, and (2) a periodical sinusoidal signal $P_{des} = 100 + 10\sin(\pi t/2)$ kPa. The 2% uncertainty variations in expression (10) and an external disturbance $\tau_d = 5\sin(2\pi t)$ kPa are considered to study the control robustness of the proposed controller. In addition, for comparison purposes, a TLSMC controller is designed by setting the sliding variable to $s = \dot{e}_p + c_1 e_p$ and the control law to $u_{tlsmc} = (b_0 - a_0 c_1)\dot{e}_p + a_0\left(\ddot{P}_r + slaw\right) + b_0\dot{P}_c + F_{sn0} + F_{rn0})$ [39], in which slaw indicates the trending law and $slaw = \dot{s}$. A PID controller is also designed with $u_{pid} = 10e_p + 0.8\dot{e}_p + F_{sn0} + F_{rn0}$ as a comparison. The nominal parameter values of the PSV are listed in Table 2, then a_0, b_0, c_0, F_{sn0} and F_{rn0} can be calculated. The parameters of the F-FTSMC controller are selected as: $c_1 = 15$, $c_2 = 20$, $q = 3$, $p = 5$, and $\gamma = 200$.

Fig. 4 shows the pressure control performance of the PSV with three controllers in case (1) and each step of the reference command lasts for 2 s, as shown in Fig. 4(a). Fig. 4(a) also shows that the actual pressures with the three controllers can track the desired pressure command well. The settling time of either the rising edge or the falling edge is approximately 0.40 s with the proposed F-FTSMC controller, while the settling time is 0.42 s with TLSMC controller and 0.48 s with the PID controller, which is slightly longer than the value for the F-FTSMC controller. The near-zero steady-state error with the F-FTSMC and TLSMC controllers can be observed in Fig. 4(b), but more tracking error is obviously observed with the PID controller. The control input u shown in Fig. 4(c) changes to track the desired pressure when the command changes. There is severe chattering of the control input with the TLSMC controller, which is greatly reduced with the F-FTSMC and PID controllers.

Fig. 5 shows the variation of the sliding variables in the F-FTSMC and TLSMC controllers. The sliding variable s of the two controllers converges to zero at a very fast convergence rate so that the control stability can be guaranteed. Besides, whether the first derivative of s in the F-FTSMC controller or the variation of slaw in the TLSMC controller is negative at time 2 s to maintain consistency with the decreasing trend of s, which is clearly displayed in the zoomed picture. The other three times (4 s, 6 s and 8 s) are similar to the one at time 2 s and thus are omitted here. The variation

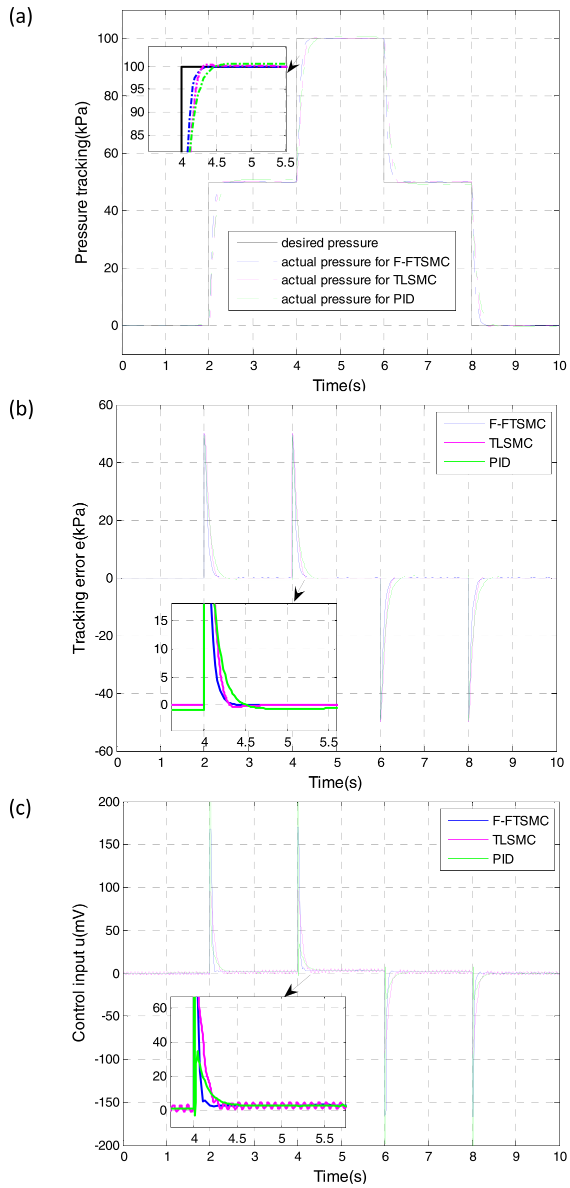

FIGURE 4. Pressure control performance of PSV with three controllers under case (1) in simulation, (a) tracking performance, (b) tracking error e_p, (c) control input u.

in the switching control coefficient μ_N in Fig. 6 is used to show the adjustment ability of the fuzzy rules designed for the F-FTSMC controller.

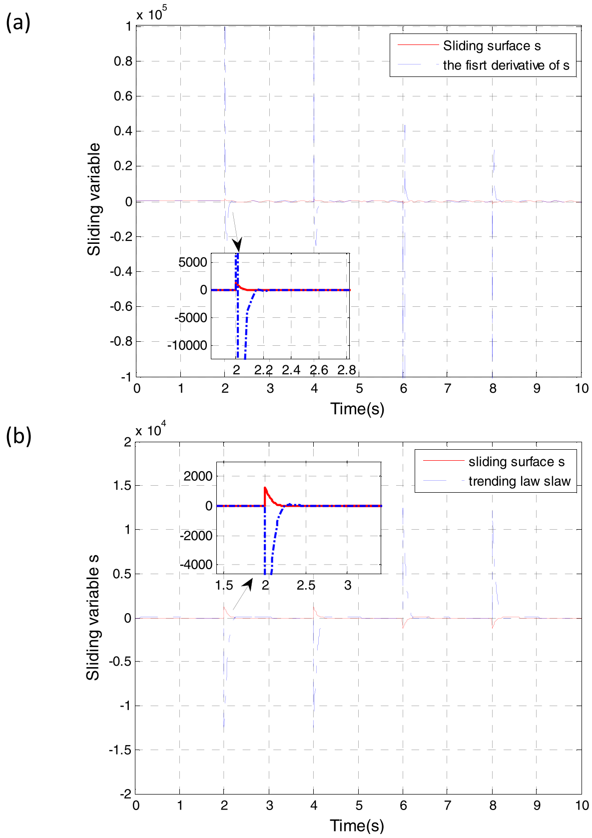

FIGURE 5. Variation of sliding variables under case (1) in simulation, (a) with F-FTSMC controller, (b) with TLSMC controller.

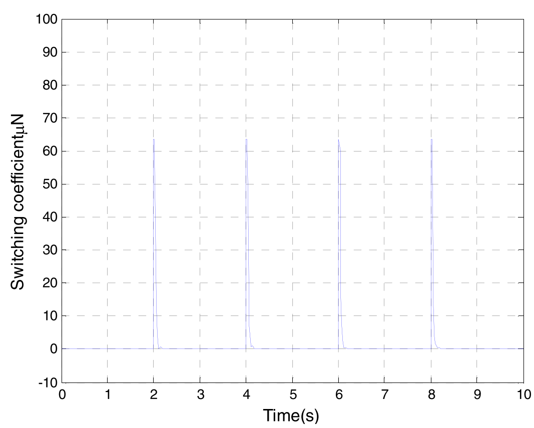

FIGURE 6. Changing of μ_N with F-FTSMC controller under case (1) in simulation.

In case (2), a sinusoidal reference command is applied to test the tracking performance of three controllers with uncertainties and external disturbances, and the simulation results are presented in Figs. 7-9. It can be easily found out from Figs. 7-8 that the proposed controller still achieves the shortest settling time (0.50 s) and the smallest steady-state tracking error. Although the tracking precision can also be ensured well by the TLSMC controller, serious chattering will exist in the control input. Similar to case (1), the PID controller achieves the largest tracking error at steady-state.

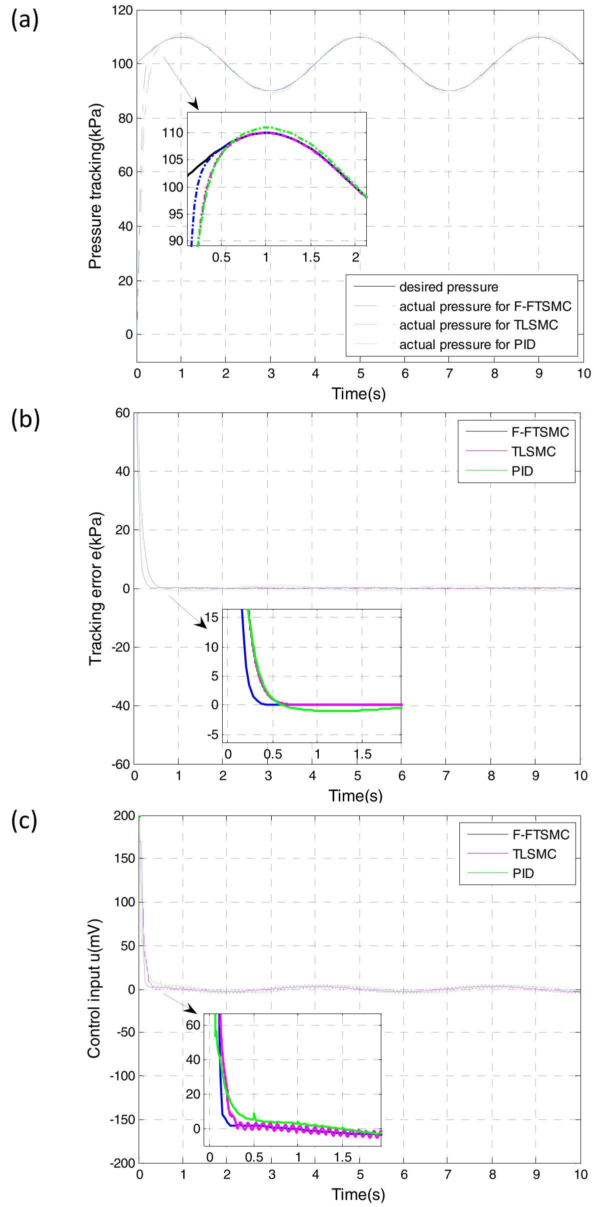

FIGURE 7. Pressure control performance of PSV with three controllers under case (2) in simulation: (a) tracking performance, (b) tracking error e_p, and (c) control input u.

In addition, the sliding variable s in Fig. 8 can converge to zero quickly to ensure a fast tracking speed, and always satisfies $s\dot{s} < 0$ and $s \cdot slaw < 0$. As shown in Fig. 9, μ_N is well tuned by fuzzy rules to reduce the chattering of the control input u in the proposed controller. The simulation results show that the proposed F-FTSMC controller can obtain faster pressure tracking with stronger robustness and smaller chattering against uncertainties and external disturbance than the TLSMC and PID controllers.

V. EXPERIMENTAL SETUP AND RESULTS

To verify the simulation results in the previous section, an experimental setup for pressure control experiments of the PSV is designed in this section and shown in Fig. 10,

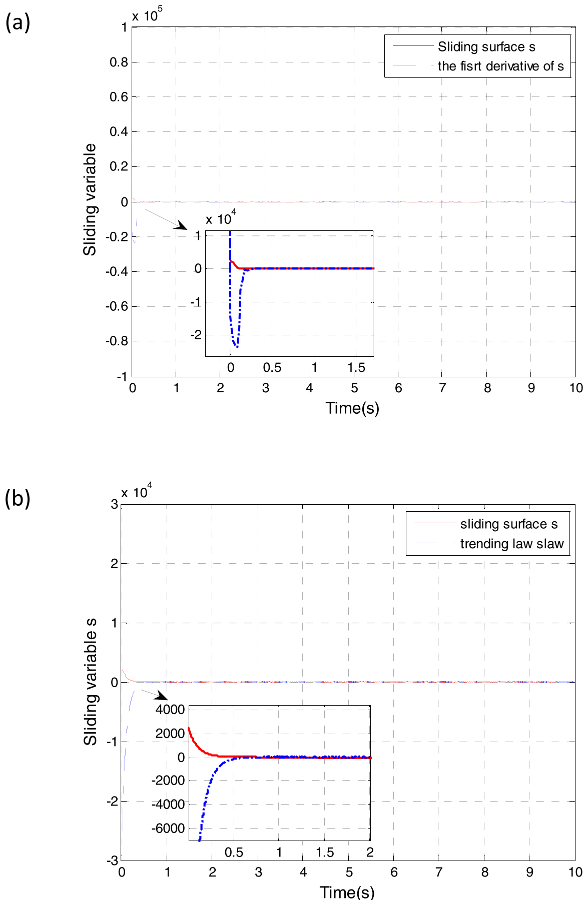

FIGURE 8. Variation of sliding variables under case (2) in simulation (a) with F-FTSMC controller and (b) with TLSMC controller.

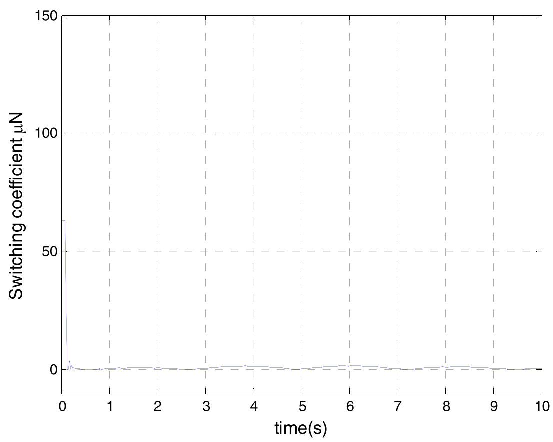

FIGURE 9. Changing of μ_N with F-FTSMC controller under case (2) in simulation.

in which only the fixture for fixing the valve is displayed due to the space limitation. The fixture introduces oil flow through different ports of the PSV, and a pressure sensor is installed at the corresponding position to measure the control pressure p_c. Besides, the oil supplied to the PSV is actuated by a motor and a pump to ensure a sufficiently large input pressure p_s. A current driving card receives the control input command and adjusts the input voltage of the PSV. In software,

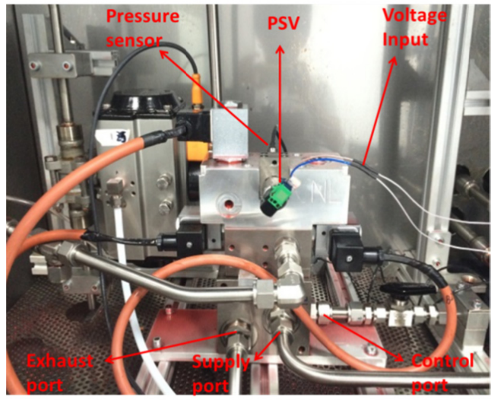

FIGURE 10. Experimental setup for pressure control experiment of PSV.

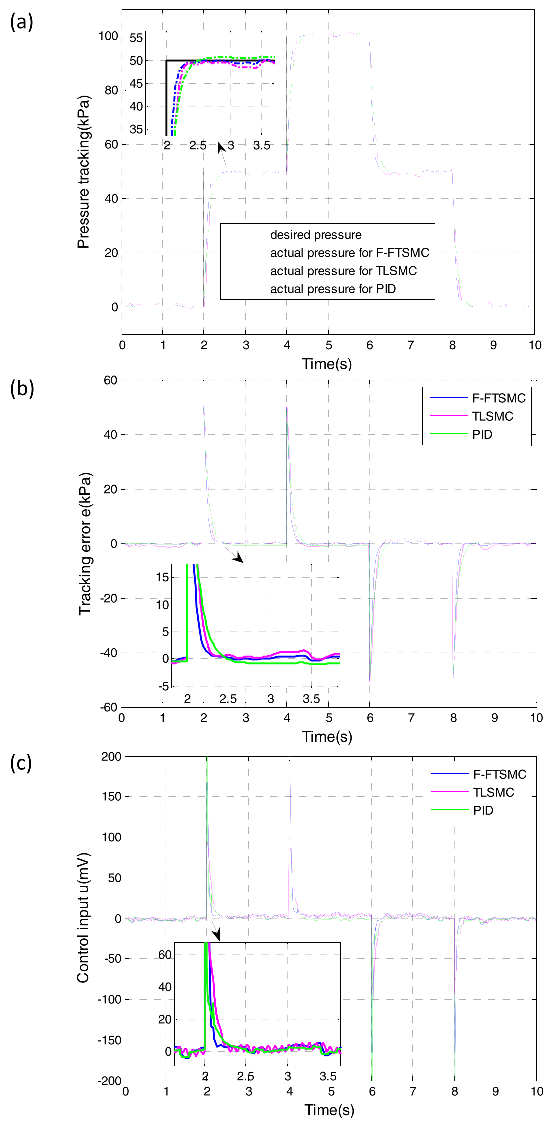

FIGURE 11. Pressure control performance of PSV with three controllers under case (1) in experiment: (a) Tracking performance, (b) tracking error e_p, (c) control input u.

NI LABVIEW is used for running the controller and data acquisition, and BECKHOFF TwinCAT is adopted to control the motor and hydraulic valve in the pipeline. The same

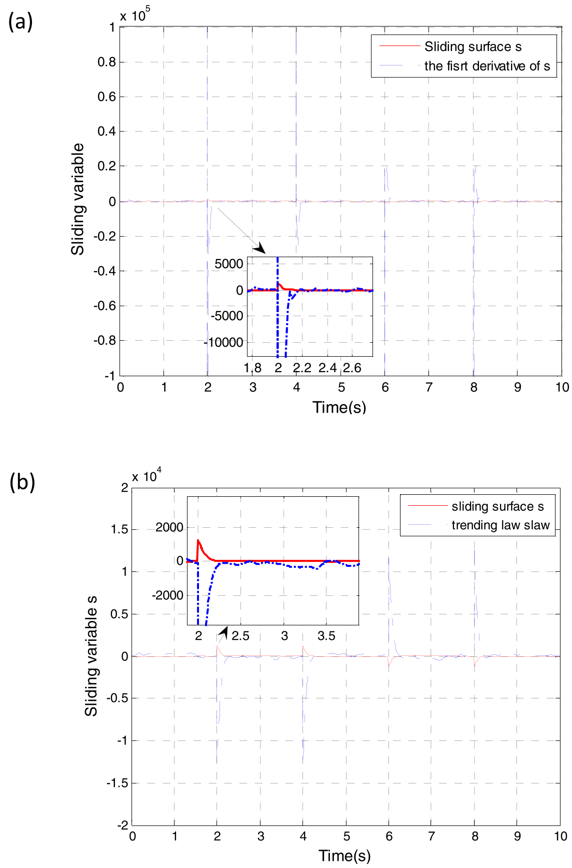

FIGURE 12. Variation of sliding variables under case (1) in experiment: (a) with F-FTSMC controller and (b) with TLSMC controller.

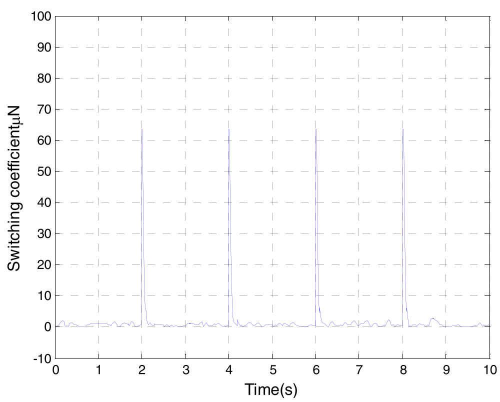

FIGURE 13. Changing of μ_N with F-FTSMC controller under case (1) in experiment.

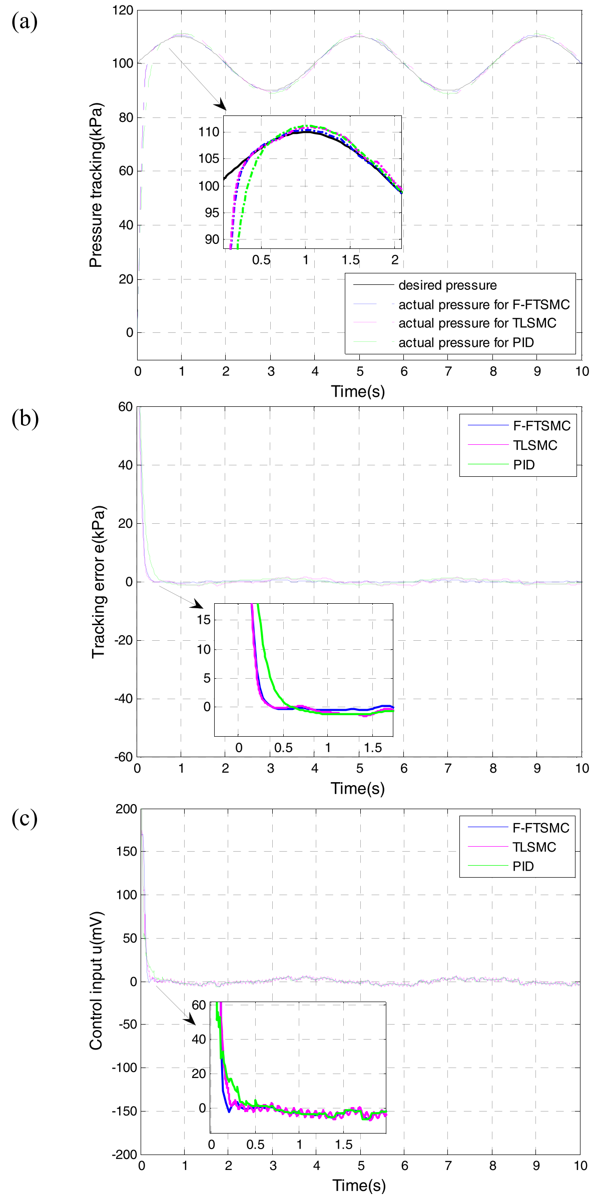

FIGURE 14. Pressure control performance of PSV with three controllers under case (2) in experiment: (a) Tracking performance, (b) tracking error e_p, and (c) control input u.

parameters of the F-FTSMC controller and the same reference commands used in the simulations are applied.

In case (1), Fig. 11 shows the pressure control performance of the PSV for the three controllers. It is obvious that the proposed controller achieves a smaller settling time than the other controllers: the settling time is approximately reduced from 0.4 s in the TLSMC controller and 0.5 s in the PID controller to 0.35 s in the F-FTSMC controller. Compared to the tracking errors of the TLSMC and PID controllers, the proposed controller achieves the smallest steady-state tracking error. By setting a value range of $e_p \in [-10, 10]$, the root mean square (RMS) values of the steady-state tracking error are calculated with the data in Figs. 11(b), and the RMS values are 0.5516, 0.9149 and 1.1694, respectively. In addition, although the tracking error in the TLSMC controller is smaller than that in the PID controller, the control input still exhibits a chattering phenomenon that will affect the performance and even the service life of the current driving card. As shown in Fig. 11(c), this chattering is apparently mitigated by the proposed controller. The variation of the sliding variables in the F-FTSMC and TLSMC controllers are also shown in Fig. 12, which all satisfy the convergence condition of sliding-mode control, that is, $s\dot{s} < 0$. In Fig. 13, the switching control coefficient μ_N is well adjusted by the F-FTSMC controller.

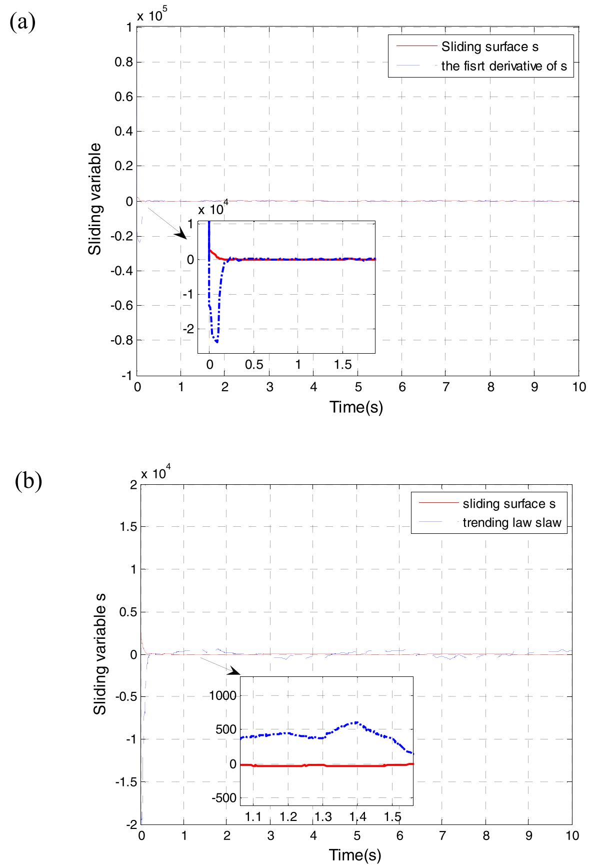

FIGURE 15. **Variation of sliding variables under case (2) in experiment: (a) with F-FTSMC controller and (b) with TLSMC controller.**

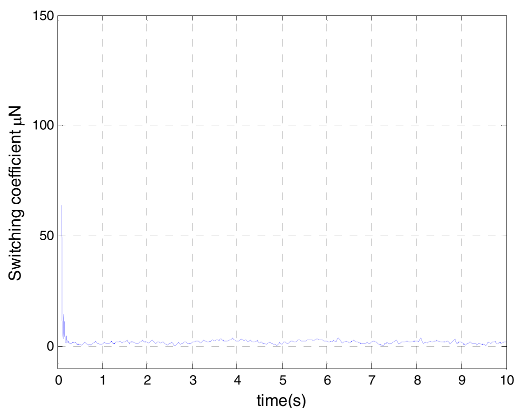

FIGURE 16. **Changing of μ_N with F-FTSMC controller under case (2) in experiment.**

In the experiment in case (2), the settling time of the pressure with the F-FTSMC controller is about 0.38 s, while the settling times are 0.42 s and 0.60 s for with the TLSMC and PID controllers as shown in Fig. 14(a). The RMS values of the steady-state errors are 1.1033, 1.3625 and 1.5689 for the different controllers shown in Fig. 14(b), respectively. Likewise, more intense chattering appears in Fig. 14(c), which is reduced by the adjustment of the fuzzy rules in the proposed F-FTSMC controller. Figs. 15-16, which show the variation of the sliding variables and switching control coefficient, all demonstrate the effectiveness of the proposed controller. Combining the results of the simulation and experiments, it has been demonstrated that the proposed F-FTSMC controller has shorter adjustment time, smaller steady-state error and less control input chattering than the TLSMC and PID controllers.

VI. CONCLUSION

In this paper, to improve the pressure tracking performance of the PSV used in the ATs of automobiles, an F-FTSMC controller is proposed to accelerate the convergence speed and eliminate the chattering of the TSMC controller. Considering the sophisticated coupling of the mechanical, hydraulic and electromagnetic characteristics inside the valve, a nominal control model of the PSV is developed to analyze its dynamic nonlinearity in the presence of uncertainties and an external disturbance. First, a fast terminal sliding surface function is designed for the TSMC controller to speed up the convergence of the sliding motion. Then, a set of fuzzy logic rules is used to tune the switching control coefficient in the control law of the FTSMC controller. Finally, the F-FTSMC controller is proposed. Although the PSV is a multidisciplinary-hybrid system, the computational complexity is reduced, and the entire controller design is organized well by analyzing different subsystems separately and some reasonable assumptions. Two different cases are studied in simulations and experiments. All the results demonstrate that the proposed F-FTSMC controller not only is highly robust to the uncertainties and external disturbance but also greatly alleviates the chattering of the control input signal. Moreover, the settling time of the pressure tracking with the proposed controller is smaller than the settling times of the other controllers considered in this paper. Future research will focus on further improving the convergence speed of the F-FTSMC controller because the convergence speed may decrease due to querying the fuzzy rules. Using local linearization techniques to express fuzzy relationships may be of interest because it can reduce the number of fuzzy control rules and thereby improve the real-time performance. In addition, other methods such as designing a state and fault observer in the switching system will be considered in the future.

ACKNOWLEDGMENT

This work was financially supported by Projects Foundation of Shanghai Science and Technology Commission, China. The authors thank F.F. Xi and S. Bao for their support and contributions to this project.

REFERENCES

[1] P. Dong, Y. Liu, P. Tenberge, and X. Xu, "Design and analysis of a novel multi-speed automatic transmission with four degrees-of-freedom," *Mech. Mach. Theory*, vol. 108, pp. 83–96, Feb. 2017.

[2] K. U. Yang, J. G. Hur, G. J. Kim, and D. H. Kim, "Non-linear modeling and dynamic analysis of hydraulic control valve; effect of a decision factor between experiment and numerical simulation," *Nonlinear Dyn.*, vol. 69, pp. 2135–2146, Sep. 2012.

[3] Q. Liu, H. Bo, and B. Qin, "Experimental study and numerical analysis on electromagnetic force of direct action solenoid valve," *Nucl. Eng. Des.*, vol. 240, pp. 4031–4036, Sep. 2010.
[4] S. Li, P. Wu, L. Cao, D. Wu, and Y. She, "CFD simulation of dynamic characteristics of a solenoid valve for exhaust gas turbocharger system," *Appl. Therm. Eng.*, vol. 110, pp. 213–222, Jan. 2017.
[5] H. Jian, W. Wei, H. Li, and Q. Yan, "Optimization of a pressure control valve for high power automatic transmission considering stability," *Mech. Syst. Signal Process.*, vol. 101, pp. 182–196, Feb. 2018.
[6] S. Wu, X. Zhao, C. Li, Z. Jiao, and F. Qu, "Multiobjective optimization of a hollow plunger type solenoid for high speed on/off valve," *IEEE Trans. Ind. Electron.*, vol. 65, no. 4, pp. 3115–3124, Apr. 2018.
[7] D. Qian, H. Mao, J. Deng, and J. Yue, "Processing optimization for large spherical valve body based on FE simulation," *Procedia Eng.*, vol. 81, pp. 2481–2487, Oct. 2014.
[8] Y. Xu, Z. Guan, Y. Liu, L. Xuan, H. Zhang, and C. Xu, "Structural optimization of downhole float valve via computational fluid dynamics," *Eng. Failure Anal.*, vol. 44, pp. 85–94, Sep. 2014.
[9] S. Corbera, J. L. Olazagoitia, and J. A. Lozano, "Multi-objective global optimization of a butterfly valve using genetic algorithms," *ISA Trans.*, vol. 63, pp. 401–412, Jul. 2016.
[10] Z. Jinsong, S. Gang, Z. Weidong, C. Yang, and Y. Jing, "Robust force control with a feed-forward inverse model controller for electro-hydraulic control loading systems of flight simulators," *Mechatronics*, vol. 38, pp. 42–53, Sep. 2016.
[11] C. Ying, Z. Jia-Fan, Y. Can-Jun, and N. Bin, "Design and hybrid control of the pneumatic force-feedback systems for Arm-Exoskeleton by using on/off valve," *Mechatronics*, vol. 17, no. 6, pp. 325–335, Jul. 2007.
[12] L. Sun and J. Zhao, "A novel adaptive backstepping design of turbine main steam valve control," *J. Control Theory Appl.*, vol. 8, no. 4, pp. 425–428, 2010.
[13] F. Meng, H. Zhang, D. Cao, and H. Chen, "System modeling and pressure control of a clutch actuator for heavy-duty automatic transmission systems," *IEEE Trans. Veh. Technol.*, vol. 65, no. 7, pp. 4865–4874, Jul. 2017.
[14] H. Wang, L. Liu, P. He, M. Yu, M. T. Do, H. Kong, and Z. Man, "Robust adaptive position control of automotive electronic throttle valve using PID-type sliding mode technique," *Nonlinear Dyn.*, vol. 85, no. 2, pp. 1331–1344, Jul. 2016.
[15] Y. Hongchang, L. Qifang, and C. Hong, "Nonlinear pressure control using triple-step method for pressure proportional solenoid valve," in *Proc. Int. Conf. Mechatronics Control (ICMC)*, Jinzhou, China, Jul. 2014, pp. 1047–1052.
[16] S. K. Chung, C. R. Koch, and A. F. Lynch, "Flatness-based feedback control of an automotive solenoid valve," *IEEE Trans. Control Syst. Technol.*, vol. 15, no. 2, pp. 394–401, Mar. 2007.
[17] C. Lv, H. Wang, and D. Cao, "High-precision hydraulic pressure control based on linear pressure-drop modulation in valve critical equilibrium state," *IEEE Trans. Ind. Electron.*, vol. 64, no. 10, pp. 7984–7993, Oct. 2017.
[18] W. Yu, D. I. Wilson, and B. R. Young, "Nonlinear control performance assessment in the presence of valve stiction," *J. Process Control*, vol. 20, pp. 754–761, Jul. 2010.
[19] X. Zhao, L. Li, J. Song, C. Li, and X. Gao, "Linear control of switching valve in vehicle hydraulic control unit based on sensorless solenoid position estimation," *IEEE Trans. Ind. Electron.*, vol. 63, no. 7, pp. 4073–4085, Jul. 2016.
[20] V. Utkin, "Variable structure systems with sliding modes," *IEEE Trans. Autom. Control*, vol. AC-22, no. 2, pp. 212–222, Apr. 1977.
[21] T. Elmokadem, M. Zribi, and K. Youcef-Toumi, "Terminal sliding mode control for the trajectory tracking of underactuated autonomous underwater vehicles," *Ocean Eng.*, vol. 129, pp. 613–625, Jan. 2017.
[22] D. Lee and G. Vukovich, "Robust adaptive terminal sliding mode control on SE(3) for autonomous spacecraft rendezvous and docking," *Nonlinear Dyn.*, vol. 83, pp. 2263–2279, Mar. 2016.
[23] Y.-J. Wu, J.-X. Zuo, and L.-H. Sun, "Adaptive terminal sliding mode control for hypersonic flight vehicles with strictly lower convex function based nonlinear disturbance observer," *ISA Trans.*, vol. 71, no. 2, pp. 215–226, Nov. 2017.
[24] H. Ma, J. Wu, and Z. Xiong, "Discrete-time sliding-mode control with improved quasi-sliding-mode domain," *IEEE Trans. Ind. Electron.*, vol. 63, no. 10, pp. 6292–6304, Oct. 2016.
[25] C.-F. Huang, T.-L. Liao, C.-Y. Chen, and J.-J. Yan, "The design of quasi-sliding mode control for a permanent magnet synchronous motor with unmatched uncertainties," *Comput. Math. Appl.*, vol. 64, pp. 1036–1043, Sep. 2012.
[26] W. Lu, C. Li, and C. Xu, "Sliding mode control of a shunt hybrid active power filter based on the inverse system method," *Int. J. Elect. Power Energy Syst.*, vol. 57, pp. 39–48, May 2014.
[27] X. Hao, X. Yang, T. Liu, L. Huang, and W. Chen, "A sliding-mode controller with multiresonant sliding surface for single-phase grid-connected VSI with an LCL filter," *IEEE Trans. Power Electron.*, vol. 28, no. 5, pp. 2259–2268, May 2013.
[28] R. Cui, L. Chen, C. Yang, and M. Chen, "Extended state observer-based integral sliding mode control for an underwater robot with unknown disturbances and uncertain nonlinearities," *IEEE Trans. Ind. Electron.*, vol. 64, no. 8, pp. 6785–6795, Aug. 2017.
[29] M. Yue, B. Liu, C. An, and X. Sun, "Extended state observer-based adaptive hierarchical sliding mode control for longitudinal movement of a spherical robot," *Nonlinear Dyn.*, vol. 78, pp. 1233–1244, Oct. 2014.
[30] V. Nekoukar and A. Erfanian, "Adaptive fuzzy terminal sliding mode control for a class of MIMO uncertain nonlinear systems," *Fuzzy Sets Syst.*, vol. 179, no. 1, pp. 34–49, 2011.
[31] Y.-J. Gu, X.-X. Yin, H.-W. Liu, W. Li, and Y.-G. Lin, "Fuzzy terminal sliding mode control for extracting maximum marine current energy," *Energy*, vol. 90, pp. 258–265, Oct. 2015.
[32] M.-J. Zhang and Z.-Z. Chu, "Adaptive sliding mode control based on local recurrent neural networks for underwater robot," *Ocean Eng.*, vol. 45, no. 1, pp. 56–62, May 2012.
[33] H. N. Al-Duwaish and Z. M. Al-Hamouz, "A neural network based adaptive sliding mode controller: Application to a power system stabilizer," *Energy Convers. Manage.*, vol. 52, pp. 1533–1538, Feb. 2011.
[34] B. S. K. K. Ibrahim, R. Ngadengon, and M. N. Ahmad, "Genetic algorithm optimized integral sliding mode control of a direct drive robot arm," in *Proc. Int. Conf. Control, Autom. Inf. Sci.*, Ho Chi Minh City, Vietnam, Nov. 2012, pp. 328–333.
[35] X. Yuan, Y. Yang, H. Wang, and Y. Wang, "Genetic algorithm-based adaptive fuzzy sliding mode controller for electronic throttle valve," *Neural Comput. Appl.*, vol. 23, no. 1, pp. 209–217, Dec. 2013.
[36] S. Mobayen, "An adaptive fast terminal sliding mode control combined with global sliding mode scheme for tracking control of uncertain nonlinear third-order systems," *Nonlinear Dyn.*, vol. 82, pp. 599–610, Oct. 2015.
[37] X. Yu, B. Wang, Z. Galias, and G. Chen, "Discretization effect on equivalent control-based multi-input sliding-mode control systems," *IEEE Trans. Autom. Control*, vol. 53, no. 6, pp. 1563–1569, Jul. 2018.
[38] V. I. Utkin and A. S. Poznyak, "Adaptive sliding mode control with application to super-twist algorithm: Equivalent control method," *Automatica*, vol. 49, pp. 39–47, Jan. 2013.
[39] B. Q. Jin, Y. K. Wang, and Y. Li Ma, "Electro-hydraulic servo system controlled by index reaching law sliding mode," *Adv. Mater. Res.*, vols. 317–319, pp. 1490–1494, Aug. 2011.

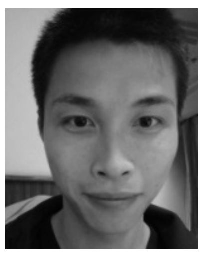

XIANGWEN FAN was born in Chuzhou, China, in 1990. He received the B.S. degree from the Institute of Mechanical and Electrical Engineering and Automation, Shanghai University, Shanghai, China, in 2012, where he is currently pursuing the Ph.D. degree in mechanical and electrical engineering through the successive master's and Ph.D. degree Program.

He has authored several articles published or reviewed. His several projects what he has participated are Automatic Testing System for Pilot Solenoid Valve in ATs, Key Technology Research and Application Demonstration of Intelligent Manufacturing of Discrete Production Lines for Auto Parts, SCARA Robot Control Software, and Development of Multi-axis Motion Control Platform for Handling Robots. His research interests include automatic control, nonlinear system modeling and dynamic characteristic analysis, adaptive robust control algorithms, and intelligent control algorithms.

YONGYI HE received the B.S. degree in mechanical engineering and automation from Chongqing University, in 1987, the M.S. degree in mechanical engineering and automation from Shanghai Technology University, in 1990, and the Ph.D. degree in mechanical engineering and automation from Shanghai University, China, in 2001.

He is a Doctoral Supervisor and the Deputy Director of the Shanghai Robotics Research Institute, Shanghai University. He has authored over 40 articles published or accepted in journals. The main projects currently undertaken include Automatic Testing System for Pilot Solenoid Valve in ATs, Key Technology Research and Application Demonstration of Intelligent Manufacturing of Discrete Production Lines for Auto Parts, SCARA Robot Control Software, Development of Multi-axis Motion Control Platform for Handling Robots, and Intelligent Research on Key Processes of Internal Components and High-efficiency Machining Process of Shaft Parts. His main research areas are robot control and application engineering, numerical control technology, and embedded control.

PENGFEI CHENG was born in Fujian, China, in 1991. He received the B.S. degree from the Institute of Mechanical and ElectronicEngineering and Automation from Shanghai University, Shanghai, China in 2012, where he is currently pursuing the Ph.D. degree in mechanical and electronic engineering through the successive master's degree and Ph.D. degree Program.

He has authored several articles published or reviewed. His projects what he has participated include Automatic Testing System for Pilot Solenoid Valve in ATs, SCARA Robot Control Software, and Development of Multi-axis Motion Control Platform for Handling Robots. His research interests include mechanical design, automatic control, and kinetics analysis and robotics.

MINGLUN FANG received the Ph.D. degree from Tsinghua University, in 1964. He studied at the University of Manchester Institute of Technology, U.K., from 1974 to 1975.

He served as the Vice President of the Shanghai University of Technology and Shanghai University, from 1986 to 2005. He has many job titles, such as the Director of the Shanghai Robotics Research Institute, the Director of Shanghai Key Laboratory of Mechanical Automation and Robotics, and the Director of the Academic Committee, Shanghai University. He is currently a Tenured Professor with Shanghai University. He is a member of the Mechanical Discipline Review Group, Academic Degrees Committee of the State Council. He has published more than 100 academic articles. His current research interests include computer integrated manufacturing systems, automation of manufacturing systems, robotics research, and application development. He presided over the development of Shanghai No. 2 Industrial Robot and won the First Prize of the Shanghai Science and Technology Progress Award. Then, he presided over the development of Shanghai No. 5 Industrial Robot and won the First Prize of the Shanghai Science and Technology Revitalization. And, the project named Auto Cylinder Head Casting Mold for Santana won the Third Prize of the Shanghai Science and Technology Progress. In addition, he was awarded the Honorary Title of Young and Middle-aged Experts With Outstanding Contributions from the State, the Excellent Teacher of Shanghai University, and Shanghai Model Worker. He has edited eight books.